NRIAG Journal of Astronomy and Geophysics (2015) 4, 179–184

National Research Institute of Astronomy and Geophysics

NRIAG Journal of Astronomy and Geophysics

www.elsevier.com/locate/nrjag

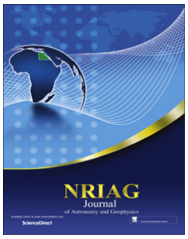

A novel technique for an integrated optical wavelength demultiplexer

M. Lotfy Rabeh [a], M. Mohanna [b,*], Tarek Hosny [a], Mohamed I. Gabr [a]

[a] *Department of Electrical Engineering, Shobra Faculty of Engineering, Benha University, Cairo, Egypt*
[b] *National Research Institute of Astronomy and Geophysics, Cairo, Egypt*

Received 4 November 2014; revised 7 July 2015; accepted 10 August 2015
Available online 3 September 2015

KEYWORDS

Laser;
Demultiplexing

Abstract In this paper we propose a new technique for optical wavelength demultiplexing (DEMUX) relaying on two phenomena: Goos–Haenchen (GH) shift and continuous refraction at a graded-index medium interface. In the first case, two light beams are totally reflected at a plane interface separating two dielectric lossless media. The reflected beams suffer different lateral shifts (GH shifts) depending on the wavelength; thus accomplishing the required spatial beam separation. In the second case, the two light beams have different "turning points" inside the graded index medium; hence, the "back-refracted" beams are spatially separated. In this paper, we optimized the conditions of operation of such demultiplexing technique. This makes possible the integration of such technique in "planar integrated-optics" structures which can be used reliably in optical fiber communication networks.

1. Introduction

Wavelength Division Multiplexing (WDM) is the optical equivalent of Frequency Division Multiplexing (FDM) to electrical signaling. WDM transmits two or more different light wavelengths in the same optical fiber. Though the process of multiplexing is reasonably straightforward, demultiplexing is much more difficult in an optical system. There are many methods (Elsenpeter and Vete, 2002; Lan, 2007; Makkerjee, 2006; Ellinas et al., 2012) to demultiplex optical signals: prisms, diffraction grating, arrayed waveguide grating (AWG), thin-film filters and interferometers. These methods vary in their relative complexities, reliability and performance. This is why optical network component manufactures try to find out simpler and more reliable techniques for demultiplexing, especially dedicated to integrated-optics architecture, because that architecture can be integrated very easily in fiber optic networks (the dream of all optical networking engineers). Consequently, we propose in this paper a novel technique which can be realized by two different methods as shown in Fig. 1.

In the first method, the GH shift depends on the wavelength and hence when two light beams with different wavelengths are incident at the critical angle on a dielectric interface separating

* Corresponding author.
Peer review under responsibility of National Research Institute of Astronomy and Geophysics.

http://dx.doi.org/10.1016/j.nrjag.2015.08.002

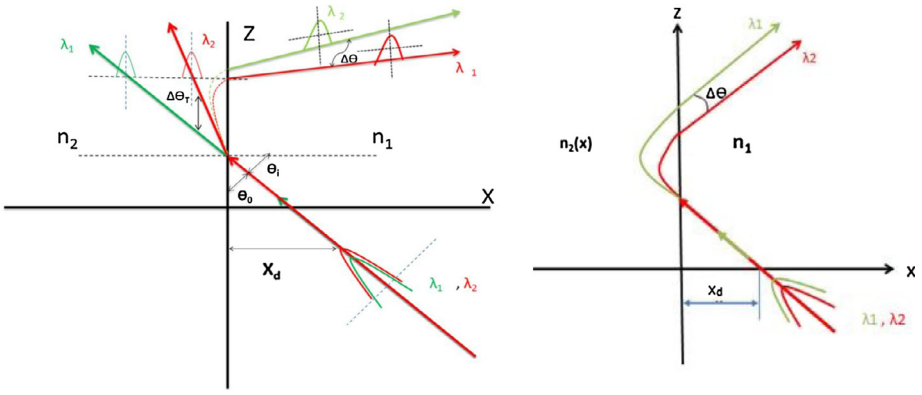

Figure 1 Optical demultiplexing at a dielectric interface.

two lossless dielectric media with refractive indices n_1 and n_2 ($n_1 > n_2$), the reflected and the transmitted beams also suffer from two different lateral shifts. Thus the separation of these wavelengths is achieved, and we are interested to optimize the separation angle $\Delta\theta$ or $\Delta\theta_T$ of the transmitted beam (due to diffraction effects) by varying the angle of incidence around the angle of incidence around the critical value ($\sin^{-1}(n_2/n_1)$). In the second method, the rarer dielectric medium n_2 is made graded-index (i.e. $n_2(x)$). Accordingly, the two light beams incident from the medium n_1, vary their penetration depth and hence reach two different "turning points" in the graded-index medium $n_2(x)$. We tried different graded "profiles" to maximize the separation angle $\Delta\theta$.

2. The beam propagation method (BPM)

To assess and evaluate the performance of the proposed novel demultiplexer we have to solve a major problem: how to study the propagation of almost "realistic" light beams? that is to say: optical beams with finite "spatial extension" like Gaussian beams. Obviously, the interest in Gaussian beams relies on many facts, because the laser beams radiated from laser sources are well approximated by Gaussian beams. Also the fundamental mode in a single-mode fiber is well approximated by a Gaussian field distribution. One of the most powerful methods used to study the propagation of light beams in complex media is the BPM (Okamoto, 2006; Obayya, 2011; Feit and Fleck, 1978; Xu and Huang, 1995). The literature on the BPM is so extensive (Xu and Huang, 1995; van Roey et al., 1981; Thylen, 1983), and hence, we shall not expose the details of that method, but we shall give a brief exposition of that method. Referring to Fig. 2, the unity amplitude y-polarized Gaussian beam at $z = 0$ in the interface coordinate system (x, z) can be written as follows (Horowitz and Tamir, 1971):

$$E_y(x,0) = \exp\left[-(X - X_d)\cos\theta_0/w\right]^2 \cdot \exp[jk_1(x - x_d) \times \sin\theta_0 \quad (1)$$

where x_d is the displacement of the beam axis from the z-axis (c.f. Fig. 2) and the time dependence $e^{-j\omega t}$ is suppressed. The BPM, first introduced by Fleck et al. (1976), relies on the expansion of $E_y(x, 0)$ as a continuous spectrum of plane waves (i.e. a "spatial" Fourier transform). Each component of the

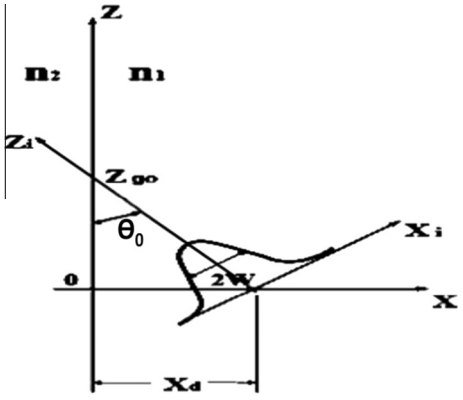

Figure 2 Gaussian beam incident at an angle $\left(\frac{\pi}{2} - \theta_0\right)$ where θ is the beam tilt angle.

spectrum is made to propagate a small distance Δz in a "homogeneous" (reference) medium having a refractive index n_0. The reference medium is usually chosen arbitrarily in the range $n_2 \leqslant n_0 \leqslant n_1$.

The propagation process is accomplished in the Fourier-domain by a single multiplication of the spatial spectrum with a phase function (propagator) which will be explained later on. After the propagation over Δz is performed, we Fourier invert the "propagated spectrum" to recover the "field" after a small distance Δz. Finally, to take into account the deviation $\delta n(x)$ of the actual refractive index distribution $n(x)$ from the value n_0, we correct the "phase" of the "propagated" field (after a small distance Δz) through a simple multiplication by $e^{-jk_0\delta n(x)\cdot\Delta z}$ to get finally the field after a propagation distance Δz.

This procedure is summarized as follows:

1. Calculate $f\,[E_y(x, 0)]$, where "f" stands for the "spatial Fourier transform operation".
2. Multiply $f\,[E_y(x, 0)]$ by a propagator operator P.
3. Calculate"f^{-1}" of the propagated spectrum obtained in step 2.
4. Apply "Q" on the field obtained in step 3, where Q represents an operator which takes into account the deviation of the actual refractive distribution $n(x)$ from the "reference value n_0".

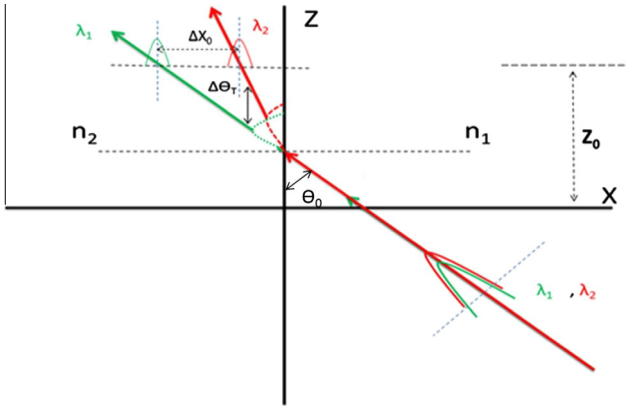

Figure 3 Two Gaussian beams at λ_1 and λ_2 incident at angles around the critical value on the interface $x = 0$.

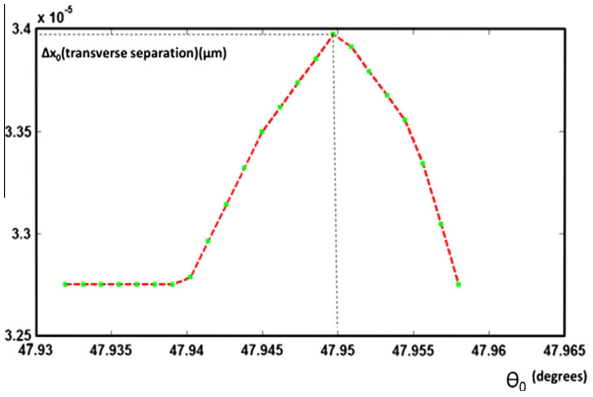

Figure 4 Transverse separation of the transmitted beams as function of beam tilt angle θ_0.

Hence, the procedure described by the previous four steps allows the calculation of $E_y(x, \Delta z)$ once $E_y(x, 0)$ is known. This means that this procedure can be repeated to calculate the total field at certain distance Z once the initial field at $z = 0$ is known. The details of the procedure are outlined in Appendix A.

3. Results for plane interface

The situation depicted in Fig. 1(a) is considered. Two Gaussian beams at wavelengths of 1.55 μm and 1.33 μm are incident at the angle $\left(\frac{\pi}{2} - \theta_0\right)$ where θ_0 is the tilt angle of the beams as shown in Fig. 3. The angle of incidence is varied in close vicinity around the critical value $\sin^{-1}(n_2/n_1)$ where we take $n_1 = 1.5$ and $n_2 = 1$. The peaks of the transmitted beams at the end of the propagation distance z_0 are separated by a distance ΔX_0 due to the wavelength dependence of the GH shift, and hence its impact on the transmitted beams can be explained with reference to Fig. 3 as follows.

The spectral components (i.e. the plane wave components) of the Gaussian beams at λ_1 and λ_2 have two parts: below the critical angle $\theta_c = \sin^{-1}(n_2/n_1)$ and above θ_c. The components below θ_c will constitute the transmitted beams at λ_1 and λ_2, while those at and above θ_c will constitute the reflected beams. We varied the angle of incidence $\left(\frac{\pi}{2} - \theta_0\right)$ around θ_c and determined ΔX_0 after $z_0 = 3000$ μm (the total propagation distance).

Fig. 4 shows that the peak of $\Delta X_0 = 34$ μm occurs at a tilt angle $\theta_0 = 47.95°$; hence, the optimal transverse separation distance ΔX_0 is – as expected – close to $\theta_0 = 48.19°$ (which is corresponding to $\theta_c = \sin^{-1}(1/1.5) = 41.81°$). This agrees with the explanation given above.

4. Results for graded-index interface

The situation depicted in Fig. 1(b) is considered where $n_2(x)$ is a graded-index distribution as shown in Fig. 5. The beam width W is taken to be equal to 10 μm and $x_d = 20$ W (c.f. Figs. 1(b) and 2).

The exponential profile $n_2(x)$ is taken as

$$n_2(x) = n_1 e^{(0.0028x)} \quad -2000\ \mu\text{m} \leqslant x < 0 \tag{2}$$

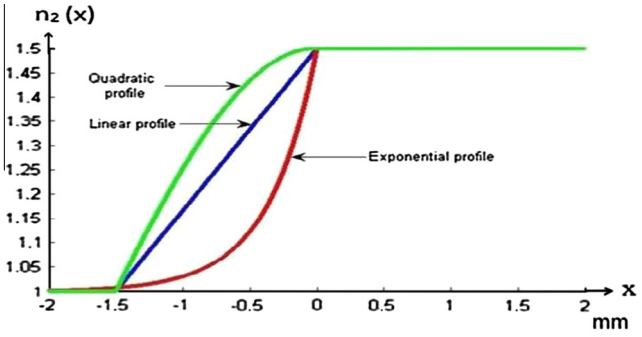

Figure 5 Types of graded indices in the region $x < 0$.

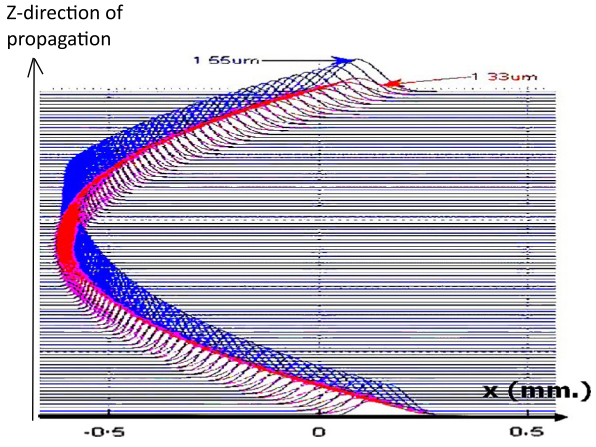

Figure 6 Gaussian beams propagating in graded index medium.

where $n_1 = 1.5$ and x is in μm and extends in the –ve direction.

The linear profile is taken as

$$n_2(x) = mx + n_1 \quad -1500\ \mu\text{m} \leqslant x < 0 \tag{3}$$

where

$$m = \frac{n_1 - n_2}{1500\ \mu\text{m}} \quad \text{Is the straight line slope} \quad (n_1 = 1.5, n_2 = 1)$$

And finally, the quadratic profile is taken as

$$n(x) = n[1 - (\alpha x)^2] \quad -2000\ \mu\text{m} \leqslant x < 0 \tag{4}$$

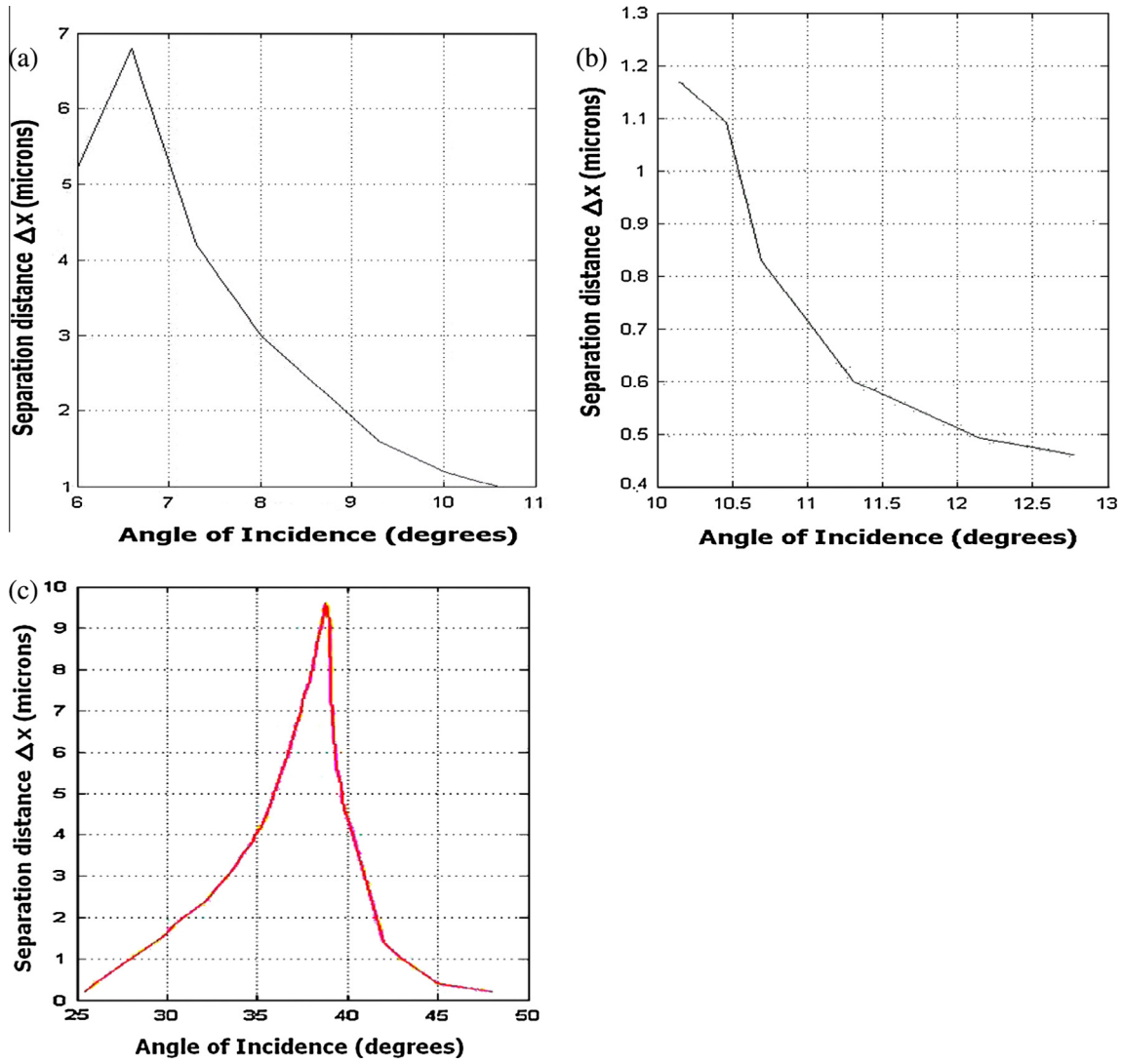

Figure 7 Variation of the transverse separation distance as function of the incidence angle for the (a) linear, (b) quadratic and exponential (c) profiles.

where X is in μm and $\alpha = 385 * 10^{-6}$ to guarantee that $n_2(x)$ varies from 1.5 at the interface $x = 0$–1 at $x = -1500$ μm (the half width of the computational window). Fig. 6 shows a sample of the BPM calculations corresponding to the linear profile. The figure reveals the "continuous refraction" of the two beams as they propagate in the graded index medium until the "turning points" are reached, where the two beams propagate back to the homogeneous medium n_1 where they are clearly separated.

As we mentioned before, we searched for the optimum angle of incidence which results in a maximum transverse separation distance Δx_0. Fig. 7 shows that there is always an optimum angle of incidence which results in maximum transverse separation distance Δx_0 as expected earlier.

5. Conclusion

In this paper we demonstrated theoretically the feasibility of a novel technique for optical Wavelength Division Multiplexing (WDM). To our knowledge, we think that this is the simplest technique in the existing literature on WDM. The technique can be realized reliably in planar integrated optic structures, and this will be more preponderant than many other existing techniques in such structures, since the integration of our proposed method in semiconductor laser diode technologies and high speed optical detectors is straightforward. The realization of the proposed method can be extended to low loss active substrates and this can open the door to many devices extremely useful in optical switching, optical computing and optical memories.

Appendix A

The problem under consideration is invariant with respect to the y-coordinate; consequently $\frac{\partial^2}{\partial y^2}$ and the scalar wave equation for E_y takes the following form:

$$\left(\frac{\partial^2}{\partial x^2} + \frac{\partial^2}{\partial z^2} + k_0^2 n^2(x)\right) E_y = 0 \tag{A1}$$

where $n(x)$ is the refractive index distribution which is the function of the transverse coordinate: x. Eq. (A1) can be written as

$$\frac{\partial^2 E_y}{\partial z^2} = -[\nabla_t^2 + k_0^2 n^2(x)]E_y \tag{A2}$$

where ∇_t^2 is the transverse Laplacian $\frac{\partial^2}{\partial x^2}$. The coefficient of E_y in the right hand member of (A2) is an operator which depends only on the transverse coordinate "x" (transverse to the direction of propagation "z") and hence, a formal operator solution of (A2) for the forward propagation field at $z = \Delta z$ in terms of its value at $z = 0$ is

$$E_y(x, \Delta z) = \{\exp(i\Delta z R)\} \cdot E_y(x, 0) \tag{A3}$$

where a time dependence $\exp(-i\omega t)$ is assumed and R is the operator:

$$R = [\nabla_t^2 + k_0^2 n^2(x)]^{1/2} \tag{A4}$$

If $n(x)$ is denoted shortly by n, then the operator R can be written as

$$R \equiv \left[\nabla_t^2 + k_0^2 n^2(x)\right]^{\frac{1}{2}} = \left\{\nabla_t^2 \Big/ \left[\left(\nabla_t^2 + k_0^2 n^2\right)^{\frac{1}{2}}\right] + k_0 n\right\} + k_0 n \tag{A5}$$

If n in the dominator of the first term in the right-hand member of (A5) is replaced by a certain reference value n_0 where $n_2 \leqslant n_0 \leqslant n_1$ then the last equation can be written as

$$(\nabla_t^2 + k_0^2 n^2)^{\frac{1}{2}} \approx \{\nabla_t^2/[(\nabla_t^2 + k^2)^{\frac{1}{2}} + k]\} + k + k[(n/n_0) - 1] \tag{A6}$$

where $k = k_0 n_0$. The approximation in (A6) is valid if the maximum deviation $\Delta n_{\max}(x)$ of $n(x)$ from the reference value n_0 satisfies the following criterion:

$$|\Delta n_{\max}|(\Delta z/\lambda_0)\sin^2\theta_{\max} \tag{A7}$$

where $\theta_{\max}$ is the angle between the direction of the highest significant plane wave component in the spatial spectrum of the total propagation field and z-axis.

If $E_y(x, z)$ is written as

$$E_y(x, z) = e_y(x, z) \cdot \exp(ikz) \tag{A8}$$

then, apart from a constant phase factor $\exp(ik\Delta z)$, direct substitution from (A8) into (A3) gives

$$e_y(x, \Delta z) = \{\exp[i\Delta z(S + k_0\delta_n)\} \cdot e_y(x, 0) \tag{A9}$$

where $\delta n = n(x) - n_0$ and $e_y(x, 0)$ is the initial field distribution at $z = 0$. The operator S is defined as

$$S = \nabla_t^2/[(\nabla_t^2 + k^2)^{1/2} + k] \tag{A10}$$

The exponent in the right-hand member of (A9) is in fact the product of two operators:

$$[\exp(i\Delta z S)] \cdot [\exp(i\Delta z k_0 \delta n 0] \tag{A11}$$

These operators do not commute; hence, an approximation is indispensable to evaluate the right-hand side of (A9). It can be shown that to second order in Δz, Eq. (A9) can be written in a symmetric split-operator form as

$$e_y(x, \Delta z) = \{P \cdot Q \cdot P\} \cdot e_y(x, 0) + O(\Delta z)^3 \tag{A12}$$

where $O(\Delta z)^3$ is a negligible term of the order of $(\Delta z)^3$ and P and Q are the two operators:

$$P = \exp[i(\Delta z/2)S] \tag{A13}$$

$$Q = \exp(i\Delta z k_0 \delta n) \tag{A14}$$

The operation $\{P\}$ ṡ $e_y(x, 0)$ represents the propagation of the initial field $e_y(x, 0)$ for a distance equal to half the step size $\Delta z/2$ in a homogeneous medium having a constant refractive index n_0, i.e. it is equivalent to solving the Helmholtz wave equation:

$$\left(\frac{\partial^2}{\partial x^2} + \frac{\partial^2}{\partial z^2} + k^2\right)E_y = 0 \tag{A15}$$

with $E_y(x, 0)$ as an initial condition at $z = 0$. Therefore advancing $E_y(x, 0)$ by repeated application of (A12) allows us to obtain the total propagating field $E_y(x, 0)$ at any distance z once the initial field is known. The operation $\{P\}$ ṡ $e_y(x, 0)$ is easily performed in Fourier space because the spatial Fourier transform of $\{P\}$ ṡ $e_y(x, 0)$ can be written as

$$F\{P \cdot e_y(x, 0) = \Psi(k_x, 0) \cdot \exp\{i\Delta z/2)k_x^2/[(k^2 - k_x^2)^{1/2} + k]\} \tag{A16}$$

where $\Psi(k_x, 0)$ is the spatial Fourier transform of the initial field $e_y(x, 0)$, i.e.

$$\Psi(k_x \cdot 0) = \int_{-\infty}^{\infty} e_y(x, 0) \cdot \exp(-ik_x x)dx \tag{A17}$$

Thus, advancing the initial field for a distance equal to half of the propagation step $\Delta z/2$ by performing the first operation $\{P\}$ ṡ $e_y(x, 0)$ in Fourier space (via (A16)), then returning back to the ordinary (x, z) plane by Fourier inversion to take into account the deviation of the actual refractive index distribution $n(x)$ from the reference value n_0 we multiply the propagated field by the correcting operator Q defined in (A14). Then, again the propagation process over the other half $\Delta z/2$ of the propagation step was performed. Repeated application of these processes allows us to calculate the total propagation field at any distance z. The Fourier transform is calculated numerically from the sampled field values at "N" discrete points x_m where $m = 1, 2, \ldots, N$, i.e. a Discrete Fourier transform (DFT) which is calculated by the Fast Fourier Transform algorithm (FFT). Accordingly, the discretized version of (A17) is written as

$$\Psi(k_{xm}, 0) = \sum_{j=-(N/2)+1}^{N/2} e_y(j\Delta x, 0) \cdot \exp(-ik_{xm} j\Delta x) \tag{A18}$$

where the spacing Δx between the samples of the field values is calculated from

$$\Delta x = L/N \tag{A19}$$

where "L" is the length of the computational region along the x-axis. The variable of the DFT (the transverse wavenumber) K_{xm} is given by

$$k_{xm} = 2\pi m/L \tag{A20}$$

From (A19) and (A20), we can write (A18) as

$$\Psi(k_{xm}, 0) = \sum_{j=-(N/2)+1}^{N/2} e_y(j\Delta x, 0) \cdot \exp(-i2\pi mj/N) \tag{A21}$$

The propagation process between $z = 0$ and $z = \Delta z$ can be summarized as follows:

1. Calculating the initial spectrum $\Psi(k_{xm}, 0)$ from field values $e_y(j\Delta x, 0)$ at N discrete points using the FFT algorithm.
2. Propagating the initial spectrum over a half step $\Delta z/2$ in the Fourier domain using (A16).
3. Fourier inverting the propagated spectrum using the inverse FFT algorithm to recover the uncorrected field after a half step.
4. Making the phase correction by multiplying the uncorrected field with the operator Q.
5. Repeating the propagation process over the half of the propagation step as described in the first two steps to obtain finally the field at $z = \Delta z$.

The previous scheme is repeated until we reach any desired propagation distance Z_{tot}. A crucial question regarding the spatial sampling interval Δx is as follows: how to choose it? It is known that as the sampling interval Δx decreases, the resolution of the spatial Fourier spectrum is enhanced. This means that higher spatial frequencies in the spectrum can be "viewed", i.e. the "fine details" of the field are enhanced. The spectrum of the incident field is centered around $k_{xi} = -\sin\theta_i$, and its maximum significant width is $\Delta k_{xi} = 4\cos\theta_i/W$ and hence the maximum deviation from k_{xi} is $\pm 2\cos\theta_i/W$.

From (A20) the maximum value of the transverse wavenumber $K_{x\max}$ in the DFT corresponds to $m = N/2$, from (A19) we can have

$$k_{x\max} = \pi/\Delta x \tag{A22}$$

Taking into account the maximum deviation of K_x around K_{xi}, an acceptable for the maximum value of the transverse wavenumber is

$$k_{x\max} = k_{xi} + (2\cos\theta_i/W)]$$

From (A22), we deduce

$$(\pi/\Delta x) = k_{xi} + (2\cos\theta_i/W) \tag{A23}$$

This means that the sampling interval Δx should not exceed the upper limit $\pi/[k_{xi} + (2\cos\theta_i/W)]$; otherwise, the high spatial frequencies in the spectrum would not be "viewed", i.e. the "fine details" of the field would be lost. Thus an acceptable upper limit on the sampling interval Δx is

$$\Delta x_{\max} \leqslant \pi/[k_{xi} + (2\cos\theta_i/W)] \tag{A24}$$

Thus the actual sampling interval Δx must be less than $\Delta x_{\max}$, for example 0.5–0.25 of that value. Finally, it is worthy to point out that the propagating field that reaches the boundary of the computational window whose width is "L", will appear as a fictitious field reflected from the boundary of that window and cause aliasing. To prevent this numerical problem, an "absorber" is put near the edges of the computational window. A wide variety of absorbers exist and are extensively used. We used a "Hanning" truncation function as an absorber, which is defined as

$$A(x) = 0.5\{1 - \cos[2\pi(x - x_d)/L]\} \quad 0 \leqslant x \leqslant L \tag{A25}$$

References

Ellinas, G., Antoniades, N., Roudas, I., 2012. WDM System and Networks. Springer, NewYork.

Elsenpeter, Robert C., Vete, Toby J., 2002. Optical Networking. McGraw-Hill/Osborne.

Feit, M.D., Fleck Jr., J.A., 1978. Light propagation in graded-index optical fibers. Appl. Opt. 17 (24), 3990–3998.

Fleck, J.A., Morris, J.R., Feit, M.D., 1976. Time-dependent propagation of high energy laser beams through the atmosphere. Appl. Phys. 10, 129–160.

Horowitz, B.R., Tamir, T., 1971. Lateral displacement of a light beam at a dielectric interface. J. Opt. Soc. Am. 61 (5), 586–594.

Lan, Cedric F., 2007. Passive Optical Networks. Academic Press.

Makkerjee, B., 2006. Optical WDM Networks. Springer, Berlin.

Obayya, Salah, 2011. Computational Photonics. John Wiley &Sons, Ltd. Publication.

Okamoto, Katsunari, 2006. Fundamentals of Optical Waveguides, second ed. Academic Press.

Thylen, L., 1983. The beam propagation method: an analysis of its applicability. Opt. Quant. Electron. 15, 433–439.

van Roey, J., van der Donk, J., Lagasse, P.E., 1981. Beam propagation method: analysis and assessment. J. Opt. Soc. Am. 71 (7), 803–810.

Xu, C.L., Huang, W.P., 1995. Finite difference beam propagation methods for guide-wave optics. Prog. Electromag. Res., PIER 11, 1–49.